DD

INSTITUTE FOR HIGH ENERGY PHYSICS

IHEP 94-94

S.A.Akimenko, V.I.Belousov, B.V.Chujko, A.A.Derevschikov, S.V.Erin, V.A.Kachanov, A.S.Konstantinov, I.V.Kotov, V.I.Kryshkin, N.G.Minaev, A.A.Morozov, A.I.Mysnick, A.I.Ronzhin, V.L.Solovianov, V.I.Shelihov, K.E.Shestermanov, O.D.Tsay, A.N.Vasiliev

Study of Strip/Fiber Prototype Shower Maximum Detector for the STAR Experiment at RHIC

Submitted to *Prib. i Tekhn. Eksp., NIM*

Protvino 1994

UDK 539.1.083.91 M-24

Abstract

Akimenko S. et al. Study of Strip/Fiber Prototype Shower Maximum Detector for the STAR Experiment At RHIC: IHEP Preprint 94-94. – Protvino, 1994. – p. 13, figs. 11, tables 1, refs.: 8

We describe the design and performance of a prototype shower maximum detector based on a two-dimensional scintillation hodoscope with a fiber readout for the STAR experiment at RHIC. The main characteristics of the detector, namely, energy response, energy and position resolution, e^-/π^- rejection power, and π^0/γ separation have been measured and calculated for different detector locations (depths) inside an electromagnetic calorimeter, different detector granularities, and various methods of construction.

Аннотация

Акименко С.А. и др. Исследование прототипа детектора максимума ливня сцинтилляционного типа: Препринт ИФВЭ 94-94. – Протвино, 1994. – 13 с., 11 рис., 1 табл., библиогр.: 8.

Представлены результаты исследовния прототипа детектора максимума ливня, состоящего из двух плоскостей сцинтилляционного годоскопа с волоконным съемом информации. Основные характеристики детектора: чувствительность к минимально ионизирующей частице, энергетическое и пространственное разрешение, e^-/π^- режекция, π^0/γ сепарация, – измерены и рассчитаны для разных положений детектора внутри электромагнитного калориметра и для разных гранулярностей детектора.

Introduction

We present results on the study of the Shower Maximum Detector (SMD) based on a scintillation hodoscope with a fiber readout (strip/fiber type), for the Solenoidal Tracker at RHIC (STAR) [1]. The STAR detector with the electromagnetic calorimeter (EMC) and the SMD will have an excellent coverage in pseudorapidity and azimuth for charged particle tracking and electromagnetic energy measurement. It is well-suited to measure $W^{\pm}$'s and Z^0's, jets, e^+e^- pairs, π^0's, direct photons, and direct photon+jet events [2]. Since the STAR detector has been described in detail elsewhere [1], only a brief summary of the planned EMC is presented here.

The proposed barrel EMC (Table 1) is a lead-scintillator sampling calorimeter. It is located inside the aluminum coil of the STAR solenoid and covers $|\eta| \leq 1.0$ and 2π in azimuth, thus matching the acceptance for full tracking in the time projection chamber. At $\eta \sim 0$, the amount of material in front of the EMC is ~ 0.5 radiation lengths (X_0).

Table 1. Barrel Electromagnetic Calorimeter Parameters

Barrel Calorimeter type	$18X_0$ lead-scintillator 'EM' section
Mechanical segmentation:	60 azimuthal sectors,$\Delta\phi = 0.105$ (6^0) 40 projective towers in $\|\eta\| < 1.0$ $\Delta\eta = 0.05$
Inner radius:	2.22 m
Length:	6.20 m
Weight:	172.7 tons
Readout:	Waveshifting fiber (2/tile) to PMT
Towers:	1,200

A detector with fine spatial resolution (SMD) will be placed into the EMC to allow for the detection of direct photons. Its goal will be to reject background photons emanating from decaying $\pi^0 \rightarrow \gamma\gamma$ or $\eta^0 \rightarrow \gamma\gamma$ mesons on the basis of the transverse shower profile. The ability to extract $W^{\pm}$ signals depends on the detector capability to distinguish hadrons from electrons. A measurement of the lateral profile of the electromagnetic shower and energy deposition in the EMC may allow for a discrimination between hard positrons/electrons from $W^{\pm}$ decays and misidentified high-p_T charged hadrons [2].

We discuss here the measurements of the energy and position resolution for different SMD methods of construction and different locations of the SMD inside the EMC. The electron/hadron rejection power for a longitudinally segmented EMC and a nonsegmented EMC with the SMD was measured. The separation of γ's from π^0 decay from single or direct-γ's was studied using the SMD with different granularities positioned at several depths inside the EMC.

1. SMD parameters and experimental setup

The requirements listed above have led to the choice of a two-dimensional scintillation hodoscope with fiber readout as a possible option of the SMD for STAR. During 1992-1994 [3] four strip/fiber prototypes of the SMD were designed, constructed and tested with electron and hadron beams at the U - 70 accelerator in Protvino. These four detectors differ from each other by granularity, construction method and absolute light yield. The active element in each hodoscope is a scintillation rod with a groove on its corner where a wave-length shifting (WLS) fiber with the diameter of 1 mm is embedded; (see Fig. 1). A WLS fiber with K27 dye (λ=490 nm), produced at INR, Russia, was used. The scintillator and the WLS fiber were wrapped with an aluminum foil. The light collected by the WLS fiber was transported via a $\sim$ 5 m long clear fiber to a FEU-85 photomultiplier, with the average quantum efficiency $\sim$ 7% at λ=490 nm. The first three detectors had scintillation strips 5 mm thick and 10, 12 and 14 mm wide. All of them had a light yield of $\sim$2.0 photoelectrons per minimum ionization particle (pe/MIP). In the fourth detector the light from the scintillation strip was collected and transported to a PMT through two WLS fibers $\sim$0.5 m long each. As a consequence it had the light yield of $\sim$7.5 pe/MIP. The thickness and the width of the scintillation strip in this detector were 5 mm and 12 mm, correspondently.

The measurements were carried out with 26.6 GeV electron and 39 GeV π^- beams. Fig. 1 shows a schematic view of the experimental setup. The size of the beam was defined by a telescope of scintillation counters $S_1 \cdot S_2 \cdot S_3 \cdot S_4 \cdot S_5 \cdot \bar{A}_0$

to be 5x2 mm^2. The electromagnetic part of the setup consisted of the $5X_0$ sampling calorimeter, the SMD, and the $20X_0$ calorimeter.

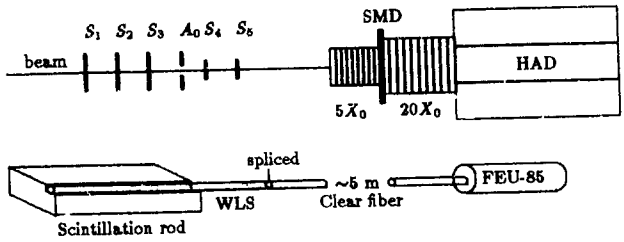

Fig. 1. Schematic view of the test setup. $S_1 - S_5, A_0$ are scintillation counters, $5X_0$ is electromagnetic calorimeter, SMD is shower maximum detector of a strip/fiber type, $20X_0$ is electromagnetic calorimeter, HAD is hadron calorimeter. Shown below is a sketch of a single element of the SMD hodoscopes, including wave-length shifting (WLS) and clear fibers, and the FEU-85 photomultiplier.

In the $5X_0$ and $20X_0$ calorimeters the light was collected through the side of the calorimeter to exclude free space between all parts of the detector. The transverse size of the $5X_0$ calorimeter was 70 mm, with a sampling of 7 layers of 4 mm thick lead alternating with 7 layers of 5 mm thick scintillator. The $20X_0$ calorimeter [4] had alternating layers of 3 mm lead and 3 mm scintillator. The transverse size was 150x150 mm^2. A compensated hadron calorimeter (HAD) was used for the identification of a beam particle and was formed from 8 modules; each module had a lateral size 100x100 mm^2. The HAD thickness corresponded to 6.0 nuclear interaction lengths, so the full calorimeter (EMC + HAD) had 7.0 nuclear interaction lengths. To obtain the dependence of the SMD performance on its location in the EMC, a noninstrumented preshower detector was used to simulate the passive material in front of the EMC. The preshower detector had sampling similar to that of the EMC planned for STAR.

2. Test results

2.1. Energy response

Fig. 2 shows a typical ADC pulse height spectrum for the SMD from 26.6 GeV electrons without the preshower detector before the SMD. The absolute light yield was determined from the detector response to these particles and was close to 2.0 photoelectrons per MIP.

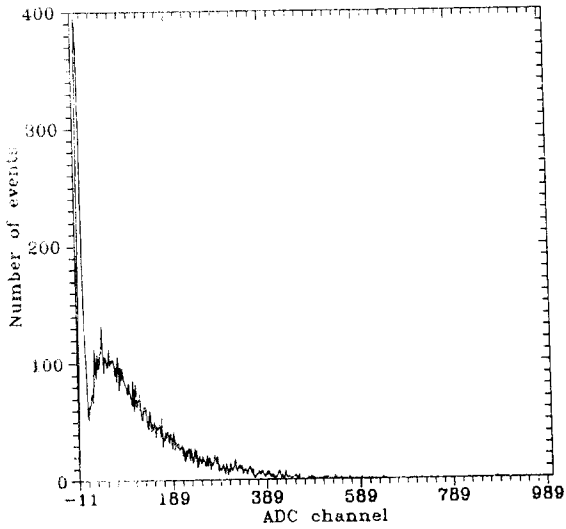

Fig. 2. Typical charge distribution for a strip/fiber assembly from 26.6 GeV electrons. The dimensions of the scintillation strip were 240x12x5 mm^3. The WLS fiber of 1 mm diameter with K 27 dye was spliced to a 5 m clear fiber. Measurements were performed with a FEU-85 photomultiplier coupled to the clear fiber. "The number of zeros" method gives $\sim$ 2.0 pe/MIP.

Once the minimum ionizing pulse amplitude was determined, all the results relating to the longitudinal shower development could be expressed in units of MIPs. Fig. 3 shows the longitudinal development of a shower initiated by 26.6 GeV electrons incident on the sandwich calorimeter, as measured and predicted by the EGS4 Monte Carlo computer program [5]. The mean ionization value as a function of the energy of an incident photon for three locations of the SMD inside the EMC is presented in Fig. 4. While the difference of the mean ionization in the SMD for showers initiated by a photon and an electron is small, the energy resolutions differ dramatically. Fig. 5 shows the energy resolution for electron data for different SMD positions inside the EMC. A similar results were obtained in [6]. Fig. 6 shows the energy resolution for photon data for three locations of the SMD and for an incoming photon energy from 0.5 to 26.6 GeV. One can see that for the SMD at $5X_0$ and an energy of an incoming e^- and γ of 26.6 GeV the energy resolution for a shower initiated by an e^- is approximately two times better than for a shower from a γ. So, to provide both a linear response and better energy resolution, the SMD should be positioned at $6.5X_0$-$7.5X_0$ inside the EMC for the energy range from 5 to 30 GeV.

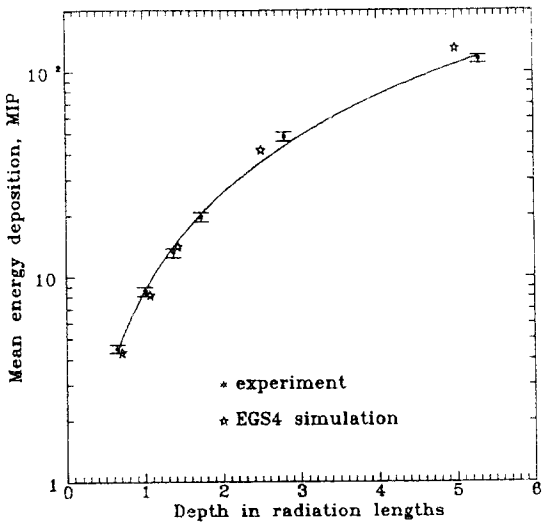

Fig. 3. The mean ionization in the SMD vs its location in the sandwich calorimeter as measured with 26.6 GeV electrons.

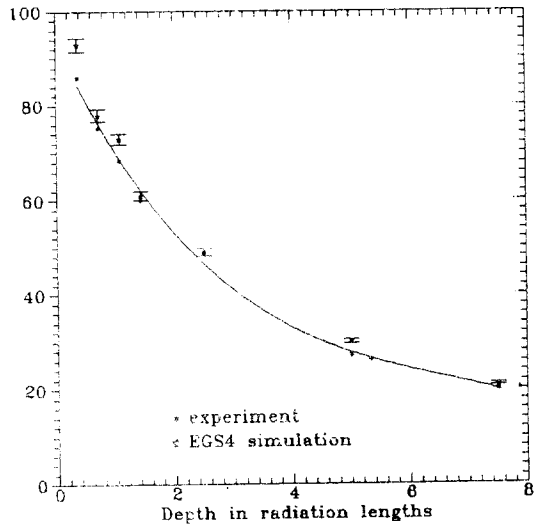

Fig. 4. The mean ionization in the SMD positioned at $3X_0$, $5X_0$, $7X_0$ as a function of the incident photons energy from the EGS4 simulation.

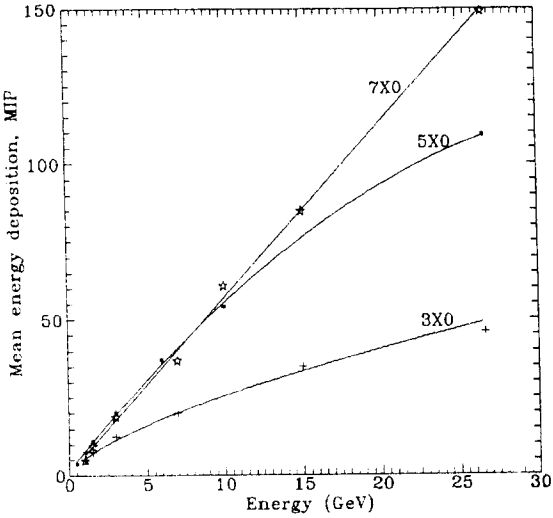

Fig. 5. Energy resolution vs the position of the SMD in the sandwich calorimeter. Showers were initiated by electrons with 26.6 GeV energy.

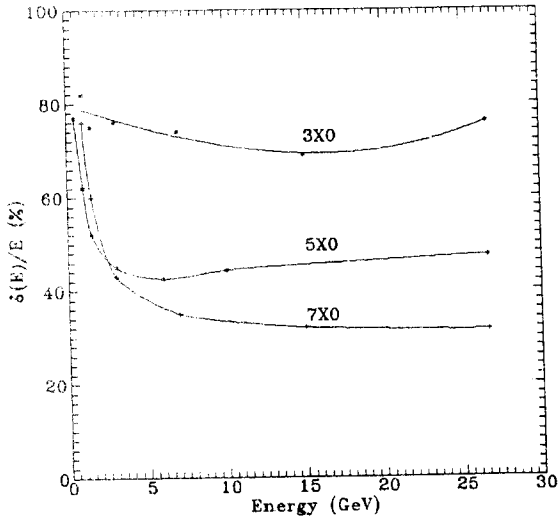

Fig. 6. Energy resolution for three positions of the SMD inside the EMC vs the incident photons energy from the EGS4 simulation.

2.2. Position resolution

The shape of the electromagnetic showers was studied by observing the fraction of the total ionization in each element of the hodoscope. Fig. 7 shows 26.6 GeV ionization distributions for the SMD with the 10 mm strips width and a detector location near $3X_0$, $5X_0$, and $7X_0$. The lateral shower density at each position was well approximated by the sum of two exponential functions. All the measurements were made for the impact point at the center of the strip. For each depth and strip width a first moment (center of gravity) calculation of the position of the electron was performed for each shower by the formula:

$$\overline{X} = \sum_{j=n_i}^{n_f} E_j \, x_j / \sum_{j=n_i}^{n_f} E_j,$$

where E_j is the energy deposition in the jth element, and x_j is the position of the center of the element. The values n_i and n_f define the strip range over which the summation has been made.

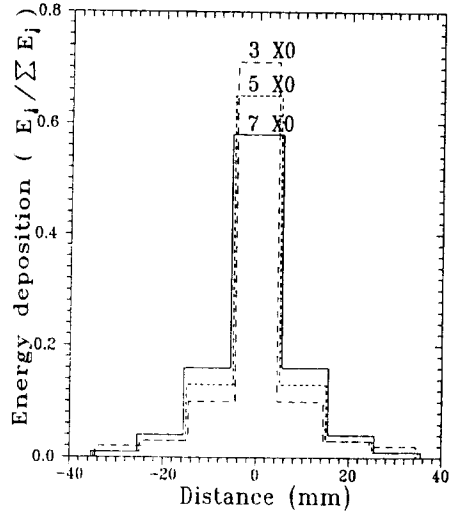

Fig. 7. Normalized energy deposition in the scintillation rods for three SMD locations in the sandwich calorimeter. Showers were initiated by electrons with the energy 26.6 GeV.

The position resolution for the SMD with the strip widths of 10 mm and 14 mm was evaluated from shower profiles and from the Gaussian fits of the distribution of $\overline{X}$. Fig. 8 shows the behavior of the position resolution for different SMD depths and strip widths. One can see that at depths close to

$7X_0$ the resolution for a 14 mm strip width is similar to the resolution for a 10 mm strip width. The position resolution for the SMD which is located deeper than $5X_0$ is insensitive to the strip summation range.

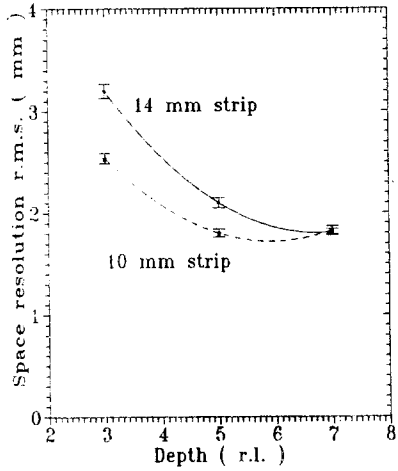

Fig. 8. Position resolution for different SMD depths and strip widths for an 26.6 GeV electrons impacting at the strip center.

Monte Carlo calculations give the dependence of the position resolution on the material inserted just before the scintillation plane. It leads to a different response for the first and the second SMD planes, due to a cut of the soft component of the shower in the first plane when the detector is located near a shower maximum. Our measurements confirm these calculations. Fig. 9 shows the first moment and the energy deposition in the scintillation plane for different materials inserted just before the scintillation rods for the SMD which is located near $7X_0$. One can see that to improve the position resolution in the second plane, a lead plate $\sim$ 2 mm thick should be positioned between the planes. Our measurement shows that albedo slightly influenced the position resolution and caused a $\sim$ 10% increase in the mean energy deposition in the scintillation plane near the shower maximum.

To obtain the influence of the light yield on the position resolution, a SMD with the $\sim$ 7.5 pe/MIP was assembled and tested. The results of the experimental study and Monte Carlo simulations show no significant difference in the response of the SMD with $\sim$ 2 pe/MIP and the SMD with $\sim$ 7.5 pe/MIP. This means that the position resolution is determined mainly by the intrinsic shower fluctuations. A similar conclusion was reached in [7]. Monte Carlo calcula-

tions also show no difference in the position resolution for a shower initiated by a photon and an electron. Fig. 10 shows the first moment vs the energy of gammas incident on the STAR EMC for different SMD locations.

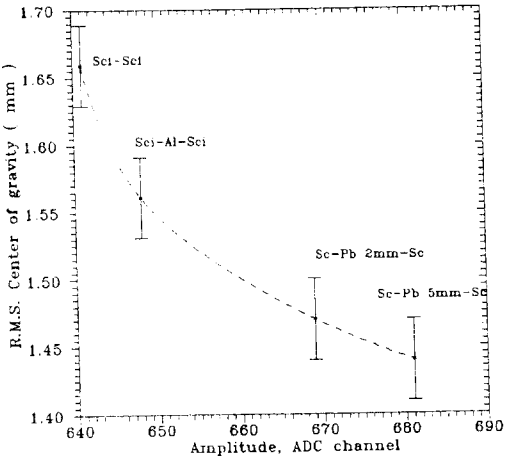

Fig. 9. First moment and energy deposition in the SMD for various materials inserted before the second SMD scintillation plane.

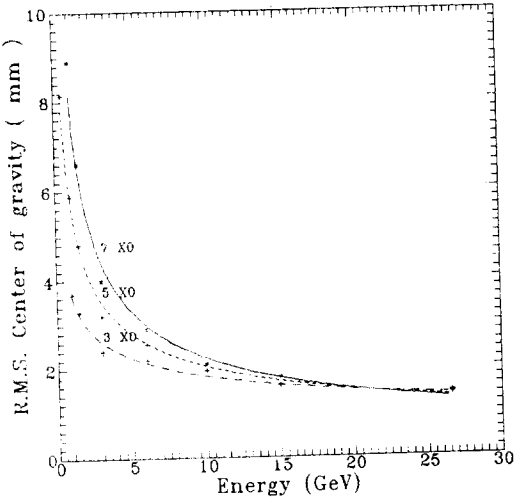

Fig. 10. First moment vs the energy of incident photons on the STAR EMC for different SMD locations from an EGS4 simulation.

We note here that the EGS4 program provides a narrower shower profile than the one obtained in the experiment. Therefore the distribution of the first moment as a result of the Monte Carlo simulations is about 20% narrower than the one measured.

Thus, we have found that the optimal parameters of the STAR SMD in terms of the position resolution and the number of SMD channels (cost) are as follows:

- strip width $\sim$ 14 mm (at η=0);
- location or depth close to $7X_0$.

2.3. e^-/π^- rejection

To compare electron/hadron rejection power for the longitudinally segmented EMC ($5X_0$+$20X_0$), the nonsegmented EMC ($25X_0$), and the nonsegmented EMC with the SMD ($25X_0$ + SMD), these detectors were tested with beams of π^- at 39 GeV and of e^- at 26.6 GeV. The rejection coefficient K was defined as the probability to identify a hadron as an electron for 90% electron detection efficiency. The $25X_0$ EMC provided a rejection at the level of $K = 1.8 \cdot 10^{-2}$. The longitudinal segmentation improved the rejection by $\sim$ 6 times and gave $K = 3.0 \cdot 10^{-3}$. The information about the energy deposition in the $25X_0$ EMC and the SMD gave $K = 5.1 \cdot 10^{-3}$. An additional study of the shower width in the SMD slightly improved the rejection, due to correlations of the SMD energy deposition and shower width, and gave $K = 4.8 \cdot 10^{-3}$.

The results listed above show that the additional information from the SMD improves the rejection power by $\sim$ 3.8 times as compared to the rejection of the nonsegmented EMC. It is poorer by $\sim$ 1.6 times as compared to the rejection of the longitudinally segmented EMC.

3. π^0/γ separation

A study has been carried out to investigate the use of the SMD to separate showers coming from a single γ from those coming from a π^0 decay. We used a procedure similar to that described in [8]. All the results were obtained for $\eta = 0$ for the STAR setup. Two parameters, the energy weighted radius $\overline{R}$ and the 'inertial moment' $E \cdot R^2$ of the shower energy deposition in the SMD, defined below, were used to find a coefficient of rejection for 90% electron detection efficiency. For every shower the parameters were calculated separately for each of the two scintillation layers of the SMD. The center of gravity of the shower

was calculated as follows:

$$X_c = \sum_{j=n_i}^{n_f} E_j \; x_j / \sum_{j=n_i}^{n_f} E_j,$$

where E_j and x_j were the energy deposition in the jth element and the coordinate of its center. The energy weighted parameter R_x was calculated as:

$$R_x = \sum_{j=n_i}^{n_f} D_{jx} \; E_j / \sum_{j=n_i}^{n_f} E_j,$$

where $D_{jx} = |X_c - x_j|$, is the distance along the x direction, of the jth element from the calculated center of gravity of the shower. For the second plate (y direction) parameters were calculated similar to those listed above.

The mean weighted radius, $\overline{R}$, was defined as follows:

$$\overline{R} = \sqrt{R_x^2 + R_y^2}.$$

The second parameter, $E\,R^2$, which provides information about the longitudinal shower development, was first calculated for each layer, and then the sum of the two moments yielded:

$$E\,R^2 = E\,R_x^2 + E\,R_y^2,$$

where, $E\,R_x^2 = \sum_j E_j\,D_{jx}^2$ and $E\,R_y^2 = \sum_j E_j\,D_{jy}^2$ were, respectively, the moments for the first and the second plates. The energy summation was taken over $\pm$ 7 cm from the calculated center of the shower.

On the scatter-plot of $E\,R^2$ vs. $\overline{R}$ the area which contains 90% of the single γ showers is marked off. Showers within this area were considered to be 'single γ's', while all showers outside this area were classified as π^0 showers. Using this definition, the probability to reject π^0's was determined for 90% single γ detection efficiency as a function of incident energy and the SMD granularity. Fig. 11 shows the result of this study. One can see that for the energy range from 10 to 30 GeV the probability to reject π^0's is weakly energy and granularity dependent. Below 10 GeV the losses of π^0's are mainly due to losses of a soft photon from highly asymmetric decays, and above 30 GeV this technique loses effectiveness since the opening angle decreases as $1/E_{\pi^0}$.

The study of the parameters defined above shows that showers initiated by γ's and π^0's are well distinguished by the use of $\overline{R}$. The additional requirement of 'inertial moment' negligibly improved the rejection power, due to the poor energy resolution of the SMD.

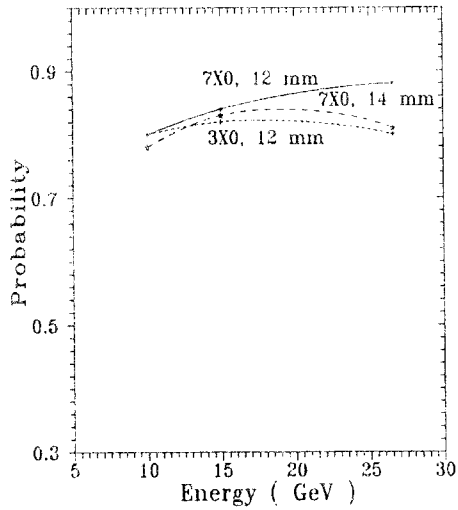

Fig. 11. π^0/γ separation for 90% γ detection efficiency as a function of π^0 energy for different SMD locations and granularities.

Conclusion

Four prototypes of scintillator strip/fiber SMDs were assembled and tested. The main characteristics of the SMDs were measured and Monte Carlo calculated. Our results show that this technique is well-suited for STAR where high rate capability, π^0/γ shower separation, good position resolution and electron/hadron rejection capability are necessary. These investigations indicate that this type SMD is a good option for the SMD for STAR.

Acknowledgements

The authors would like to thank the technical teams of the PROZA collaboration at U-70 for their assistance during the detectors assembling, in particular, Yu.Il'in, V.Kormilitsin, and V.Lavrentiev. Also we would like to thank Dr.H.Spinka from ANL (USA) for the fruitful discussions.

References

[1] Conceptual Design Report for the Solenoidal Tracker At RHIC, The STAR Collaboration, PUB-5347 (1992).

[2] Proposal on Spin Physics Using the RHIC Polarized Collider (update), R5 experiment at RHIC, September 2, 1993, Brookhaven, NY, USA.

[3] B. Chuiko et al. -IHEP Preprint 92-104, Protvino, 1992.

[4] V.I. Kryshkin, A.I. Ronzhin. Nucl. Instr. Meth. A247 (1986).

[5] W.R.Nelson, H.Hirayama, D.W.Rogers - SLAC Report 165, Stanford, SLAC, 1985.

[6] Ts.A.Amatuni et al. - IHEP Preprint 81-109, Serpukhov, 1981.

[7] V.B. Gorodnichev et al. Nucl. Instr. Meth. A343 (1994).

[8] J. Grunhaus, S. Kananov, C. Milstene - TAUP-1976-92, TelAviv University, Tel-Aviv, Israel, 1992.

Received September 8, 1994

Акименко С.А. и др.
Исследование прототипа детектора максимума ливня сцинтилляционного типа.

Оригинал-макет подготовлен с помощью системы LaTeX.
Редактор Е.Н.Горина. Технический редактор Н.В.Орлова.

Подписано к печати 12.09.1994 г. Формат 60 × 90/16.
Офсетная печать. Печ.л. 0,81. Уч.-изд.л. 1,004. Тираж 240. Заказ 24.
Индекс 3649. ЛР №020498 06.04.1992.

Институт физики высоких энергий, 142284, Протвино Московской обл.

Индекс 3649

П Р Е П Р И Н Т 94-94, И Ф В Э, 1994